



Natural Convection Heat Transfer in an Inclined Open-Ended Square Cavity with Partially Active Side Wall

Jasim M. Mahdi

Department of Energy Engineering/ College of Engineering/ University of Baghdad

E-mail: jasim_ned@yahoo.com

(Received 10 November 2011; accepted 7 August 2012)

Abstract

This paper reports a numerical study of flow behaviors and natural convection heat transfer characteristics in an inclined open-ended square cavity filled with air. The cavity is formed by adiabatic top and bottom walls and partially heated vertical wall facing the opening. Governing equations in vorticity-stream function form are discretized via finite-difference method and are solved numerically by iterative successive under relaxation (SUR) technique. A computer program to solve mathematical model has been developed and written as a code for MATLAB software. Results in the form of streamlines, isotherms, and average Nusselt number, are obtained for a wide range of Rayleigh numbers 10^3 - 10^6 with Prandtl number 0.71 (air), inclination angles measured from the horizontal direction 0° - 60° , dimensionless lengths of the active part 0.4-1, and different locations of the thermally active part at the vertical wall. The Results show that heat transfer rate is high when the length of the active part is increased or the active part is located at middle of vertical wall. Further, the heat transfer rate is poor as inclination angle is increased.

Keywords: *Natural convection, square cavity, partially active side wall.*

1. Introduction

Natural convection in a cavity with one vertical side open has received increasing attention in recent years due to its importance in a number of practical applications such as heat transfer and fluid flow in solar thermal receiver systems [1], fire spread from room [2], and cooling of electronic equipment [3]. Many theoretical and experimental studies on natural convection in the 2-D open square cavity have been carried out [4]–[10]. For the sake of brevity literature review will be only restricted to studies of natural convection in open square cavities with adiabatic walls and isothermal at the wall facing the aperture. Chan and Tien [4] performed a numerical study of laminar natural convection in a two-dimensional square open cavity with a heated vertical wall and two insulated horizontal walls. To overcome the difficulties of unknown conditions at the opening, they made their calculations in an extended computational domain beyond the opening. Results obtained for

Rayleigh numbers ranging 10^3 - 10^6 were found to approach those of natural convection over a vertical isothermal flat plate. Later on, the same authors [5] investigated open shallow cavity for Rayleigh numbers up to 10^6 to test the validity of approximate boundary conditions at the opening for a computational domain restricted to the cavity instead of using an extended domain. They concluded that for a square open cavity having an isothermal vertical side facing the opening and two adiabatic horizontal sides, satisfactory heat transfer results could be obtained by the restricted domain. Polat and Bilgen [6] numerically studied inclined fully open shallow cavities in which the side facing the opening was heated by constant heat flux, and two adjoining walls being adiabatic over Rayleigh number values ranging 103 - 1010. The opening was in contact with a reservoir at constant temperature and pressure; the computational domain was restricted to the cavity. They observed that heat transfer approaches asymptotic values at Rayleigh numbers independent of the aspect ratio and asymptotic

values are close to that for a flat plate with constant heat flux. Chakrour [7] performed an experimental investigation to study the effect of wall conditions as well as its tilt angle on heat transfer for a fully open tilted cavity.

His study contains seven different wall configurations over an inclination angle measured from the vertical direction range -90° to $+90^\circ$. It was concluded that the tilt angle, wall configuration, and number of hot walls are all factors that strongly affect the natural convection inside the fully open cavity. Nateghi and Armfield [8] numerically studied natural convection flow in a two dimensional inclined open cavity for both transient and steady-state flow over Rayleigh numbers ranging 105 - 1010 with Prandtl number 0.71 and inclination angles 10° - 90° . Their results showed that the flow is steady at the low Rayleigh number for all angles and becomes unsteady at the high Rayleigh number for all angles and the critical Rayleigh number decreases as the inclination angle increases. Hinojosa et al. [9] presented results for natural convection and surface thermal radiation in a square tilted open cavity. Effects of Rayleigh number 103 - 107 and inclination angles 0° - 180° are investigated for a fixed Prandtl number (0.7). The results show that the convective Nusselt number changes substantially with the inclination angle of the cavity, while the radiative Nusselt number is insensitive to the orientation change of the cavity.

Mohamad et al. [10] simulated the natural convection in an open cavity using Lattice Boltzmann Method. The paper demonstrated that open boundary conditions used at the opening of the cavity are reliable, where the predicted results are similar to that of conventional CFD method. Prandtl number is fixed to 0.71 while Rayleigh number and aspect ratio of the cavity are changed in the range of 104 to 106 and of 0.5 to 10, respectively. The results show that the rate of heat transfer decreases asymptotically as the aspect ratio increases and may reach conduction limit for large aspect ratio.

Most of the above-cited works deal with the active vertical wall of the cavity at isothermal or isoflux condition. In real life such as in fields like solar energy collection and cooling of electronic components, the active wall may be subject to abrupt temperature nonuniformities due to shading or other natural effects[11], therefore only a part of the wall is either in isothermal or isoflux condition. The present study deals with the natural convection in an open square cavity filled with air as working fluid with partially thermally active vertical wall, for different lengths of thermally

active part. The active part is located at the top, middle and bottom to locate the position where the heat transfer rate is maximum and minimum.

2. Mathematical Formulation

The geometry, the coordinate system, and the boundary conditions for the problem under consideration are shown in Fig. (1). A portion of the right side wall of the cavity is kept at a temperature T_h and the remaining parts are insulated. Under the assumptions of a two-dimensional viscous incompressible fluid with steady-state conditions, the equations governing the motion and the temperature distribution inside the cavity may be written as: [12]

Continuity equation

$$\frac{\partial \mathbf{u}}{\partial X} + \frac{\partial \mathbf{v}}{\partial Y} = 0 \quad \dots(1)$$

Conservation of momentum in x-direction

$$\rho \left[\mathbf{u} \frac{\partial \mathbf{u}}{\partial X} + \mathbf{v} \frac{\partial \mathbf{u}}{\partial Y} \right] = - \frac{\partial p}{\partial x} + \mu \left[\frac{\partial^2 \mathbf{u}}{\partial x^2} + \frac{\partial^2 \mathbf{u}}{\partial y^2} \right] + \rho g \sin \phi \quad \dots(2)$$

Conservation of momentum in y-direction

$$\rho \left[\mathbf{u} \frac{\partial \mathbf{v}}{\partial X} + \mathbf{v} \frac{\partial \mathbf{v}}{\partial Y} \right] = - \frac{\partial p}{\partial y} + \mu \left[\frac{\partial^2 \mathbf{v}}{\partial x^2} + \frac{\partial^2 \mathbf{v}}{\partial y^2} \right] - \rho g \cos \phi \quad \dots(3)$$

Energy Equation

$$\mathbf{u} \frac{\partial T}{\partial X} + \mathbf{v} \frac{\partial T}{\partial Y} = \alpha \left[\frac{\partial^2 T}{\partial x^2} + \frac{\partial^2 T}{\partial y^2} \right] \quad \dots(4)$$

As in many investigations of natural convection, all fluid properties, except density in buoyancy term (ρg), are assumed constants and the Boussinesq approximation is used to incorporate the temperature dependence of density in the momentum equation. In this approximation the density in buoyancy term is assumed to be a linear function of temperature, $\rho = \rho_\infty (1 - \beta(T - T_\infty))$ [12].

The use of vorticity-stream function formulation can eliminate pressure gradient terms from momentum equations and simplify the solution procedure. With the stream function, the velocity components u and v and vorticity can be expressed as:

$$\mathbf{u} = -\frac{\partial\psi}{\partial y}, \mathbf{v} = \frac{\partial\psi}{\partial x} \text{ and } \omega = \frac{\partial\mathbf{u}}{\partial y} - \frac{\partial\mathbf{v}}{\partial x}$$

Furthermore by introducing the following no dimensional variables: $(X, Y) = (x, y)/L$, $(U, V) = (\mathbf{u}, \mathbf{v})/(\alpha/L)$ $\Psi = \psi/\alpha$, $\Omega = \omega/(\alpha/L^2)$, $\theta = (T - T_\infty)/(T_h - T_\infty)$ with $T_h > T_\infty$, the governing equations in terms of vorticity-stream function form become:

Stream function

$$\nabla^2\Psi = -\Omega \quad \dots(5)$$

Vorticity

$$\nabla^2\Omega = \frac{1}{Pr} \left[U \frac{\partial\Omega}{\partial X} + V \frac{\partial\Omega}{\partial Y} \right] - Ra \left(\frac{\partial\theta}{\partial X} \cos\phi - \frac{\partial\theta}{\partial Y} \sin\phi \right) \quad \dots(6)$$

Energy

$$\nabla^2\theta = U \frac{\partial\theta}{\partial X} + V \frac{\partial\theta}{\partial Y} \quad \dots(7)$$

where

$$U = -\frac{\partial\Psi}{\partial Y} \quad V = \frac{\partial\Psi}{\partial X} \quad \dots(8)$$

The dimensionless parameters appearing in equations (5) through (8) are the Prandtl number $Pr = \nu/\alpha$ and the Rayleigh number $Ra = g\beta(T_h - T_\infty)L^3/\alpha\nu$.

Other parameters which enter into this study are the dimensionless length of the active part $H = \frac{h}{L}$ ($0.4 \leq H \leq 1$) and the dimensionless position of the active part center $S = \frac{s}{L}$ ($H/2 \leq S \leq 1 - H/2$).

The appropriate boundary conditions in dimensionless form can be formulated as:

$$\text{at } X = 0, S \leq Y \leq S + \frac{H}{2},$$

$$\Psi = 0 \quad \Omega = -\frac{\partial^2\Psi}{\partial X^2} \quad \theta = 1$$

$$\text{at } X = 0, 0 \leq Y < S - \frac{H}{2}, S + \frac{H}{2} < Y \leq 1,$$

$$\Psi = 0 \quad \Omega = -\frac{\partial^2\Psi}{\partial X^2} \quad \frac{\partial\theta}{\partial X} = 0$$

$$\text{at } 0 < X < 1, Y = 0, 1, \text{ and}$$

$$\Psi = 0 \quad \Omega = -\frac{\partial^2\Psi}{\partial Y^2} \quad \frac{\partial\theta}{\partial Y} = 0$$

$$\text{at } X = 1, 0 < Y < 1.$$

$$\frac{\partial\Psi}{\partial X} = \frac{\partial\Omega}{\partial X} = 0, \begin{cases} \theta = 0 & \text{if } U \leq 0 \text{ (inflow)} \\ \frac{\partial\theta}{\partial X} = 0 & \text{if } U > 0 \text{ (outflow)} \end{cases}$$

Local Nusselt number on thermally active part is defined by:

$$Nu = -\frac{h_y L}{k} = \frac{L}{T_w - T_\infty} \left[\frac{\partial T}{\partial x} \right]_{x=0}$$

Where the local heat transfer coefficient h_y is defined by equating heat transfer by convection to that by conduction at the active part:

$$h(T_w - T_\infty) = -k \left[\frac{\partial T}{\partial x} \right]_{x=0}$$

by introducing the dimensionless variables defined above, local Nusselt number will be:

$$Nu = \left[\frac{\partial\theta}{\partial X} \right]_{X=0}$$

The average Nusselt number is obtained by integrating local Nusselt number over the active part:

$$\bar{Nu} = \int_{S-(H/2)}^{S+(H/2)} Nu \cdot dY$$

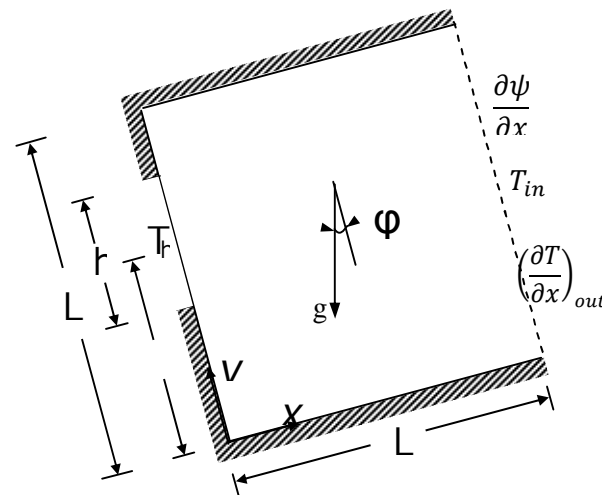


Fig. 1. Schematic of the Square Cavity, the Coordinate System and Boundary Conditions.

3. Numerical Technique

A finite difference method (FDM) with central difference scheme is used to discretize the system of the partial differential equations (5 - 8). The new algebraic equations system will be solved using iterative under relaxation method (URM), to give approximate values of the dependent variables at a number of discrete points called (grid points or nodes) in the computational domain. These nodes are formed by subdividing the computational domain in the X and Y directions with vertical and horizontal uniformly

spaced grid lines. Based on a grid independence study a grid of 61 × 61 nodes is adopted typically in this study. However, a careful check for the grid independence of the numerical solution has been made to ensure the accuracy and validity of the numerical schemes. For this purpose, four grid systems, 45×45, 61×61, 81×81, and 101×101 are tested. Results show the average Nusselt number prediction for 61×61 grid points nearly correspond to that obtained from other grid points, the maximum relative error (% ε) obtained through the five grid systems is no more than 1% as shown in Table (1). The accuracy of the numerical code was assessed by applying it to a case studied by Mohamad et al. [10], who considered a cavity configuration similar to that being considered in this paper with a fully active hot vertical wall, and good agreement was observed, as shown in Table (2). The maximum difference obtained for the average Nusselt number at the hot vertical wall was 1.7 %. Furthermore, in order to lend more confidence in the present numerical results, the results in form of isothermals contours were compared with those of Nateghi and Armfield [8] and Mohamad et al. [10]; and an excellent agreement was achieved, Fig.(2).The convergence criteria employed to terminate the computations and reach the solution were preassigned as $(\Psi^\zeta - \Psi^{\zeta-1})/\Psi^\zeta \leq 10^{-6}$, $(\theta^\zeta - \theta^{\zeta-1})/\theta^\zeta \leq 10^{-6}$, and $(\Omega^\zeta - \Omega^{\zeta-1})/\Omega^\zeta \leq 10^{-6}$, the indices ζ and $\zeta - 1$ represent the current and previous iteration, respectively.

Table 1,
Grid Independence Study Results for Average Nusselt Number.

Size	45×45	61×61	81×81	101×101	% ε
Ra = 10 ³	1.173	1.180	1.188	1.189	1.0
Ra = 10 ⁴	3.308	3.319	3.327	3.318	0.5
Ra = 10 ⁵	7.284	7.301	7.301	7.298	0.3
Ra = 10 ⁶	14.32	14.22	14.23	14.27	0.7

Table 2,
Comparison of the Obtained Results for Average Nusselt Number with Literature.

Ra	Nu [10]	Nu [this study]	Difference (%)
10 ⁴	3.377	3.319	1.7
10 ⁵	7.323	7.301	0.2
10 ⁶	14.38	14.22	1.1

4. Results and Discussion

In this section, the numerical results in form of the streamlines, isotherms, and average Nusselt numbers for various values of the parameters governing the heat transfer and fluid flow will be presented and discussed. The parameters are location of thermally active part, the dimensionless length of thermally active part, H = 0.4 - 1.0, Rayleigh number, Ra = 10³ - 10⁶, and inclination angle, φ = 0° - 60°. Prandtl number, Pr = 0.71 for air was kept constant. In Figures (3-6), the darkened area of side wall indicates the position of thermally active part while the symbol (⊕) represents the center of the circulation which defined as the point of the extremum of the stream function Ψ_{max} .

The scenario of development natural convective currents inside open cavity begins when the air in contact with the active part of side wall heated by conduction, becomes lighter, and ascends in adjoin to the side wall to face the adiabatic upper wall and then through which it moves horizontally to leave the cavity from the upper part of the aperture. In order to retrieve fluid left outside the cavity, fresh air entrained from the lower part of the aperture toward heated portion of side wall to be heated and resulting in clockwise recirculation inside cavity, as shown in left sides of Figs. (3-6).

4.1. Effect of Active Part Length

The effects of active part length H on flow and temperature fields are shown in figure (3) for Rayleigh number, Ra = 10⁵, inclination angle, φ = 0° and position of active part is at middle. The values of maximum stream functions Ψ_{max} show that higher values are obtained with increasing the active part length from H=0.4 to H=1. In fact, when the active part is wider major portion of the cavity is occupied by circulating cells (see streamlines in Fig. (3)) and flow strength increases making the cavity more significantly affected by the buoyancy-driven flow. The corresponding isotherms indicate that as H increases the isotherms are denser near the active part that means thermal boundary layer becomes thinner and temperature gradients becomes steeper due to strong convection. The amount of heat transferred from the active part across the cavity obviously increases as the length H of the thermally active part increases due to higher heat transfer surface. Correspondingly, average Nusselt number which would describe the thermal

behavior of the cavity should increase with increasing H as shown in Fig. (7).

4.2. Effect of Active Part Location

Figure (4) shows the effect of active part position on the streamlines and isotherms patterns at $Ra = 10^5$, $\varphi = 0^\circ$, and dimensionless length of active part, $H=0.4$. In fact, due to impingement of circulated fluid to the middle of the vertical wall and impingement of hot fluid to the top adiabatic wall, fluid at right top and bottom corner becomes motionless and also, the half bottom of the cavity becomes cooler than the upper one. Thus strength of circulation becomes larger, as clearly denoted by the higher value of Ψ_{max} , and major portion of the cavity is occupied by circulating cells as the active part occupies a position lower in the cavity (see streamlines in Fig. (4)). In contrast, when the active part is located at the bottom or the top of vertical wall the rising fluid by buoyancy force cannot wash the entire surface of the active part and thermal boundary layer around the active part gets thicker (see isotherms in Fig. (4)), thus the amount of heat exchanged is smaller than that exchanged when the active part is located at middle of vertical wall. Subsequently, the average Nusselt number which describes the overall heat transfer process through the cavity is higher when the active part located at middle as shown in Fig. (8).

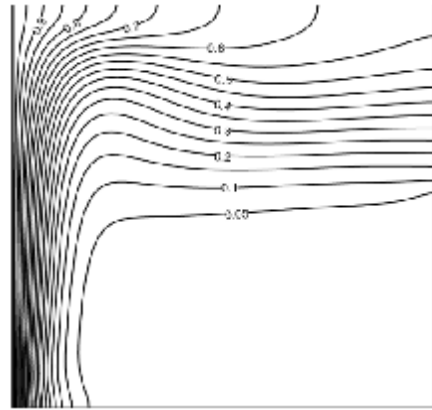
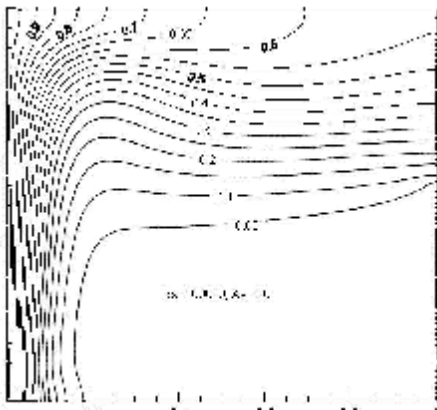
4.3. Effect of Inclination

The effect of inclination angle φ in the range of 0 to 60° which covering practical cases in solar collectors [6] is examined for $Ra=10^5$ and $H=0.6$. Fig. (5) shows the effect of inclination angle on streamlines and isotherms patterns. Streamlines show that as the inclination is increased flow of the hot fluid from the aperture is choked and a smaller part of the upper region of the cavity is occupied by discharged fluid. As a result, the center of the circulation \oplus is impelled upward indicating significant increase in fluid velocities. The isotherms show a thicker thermal boundary layer is formed on the active part of side wall, and also a thinner hot intrusion on the upper insulated wall formed as inclination angle increases. Increasing the inclination angle in the range $0^\circ \leq \varphi \leq 60^\circ$ leads to a decrease in the average Nusselt number for the same dimensionless length of active part as shown in Fig. (9). This because as φ increases, the thermal boundary layer on active part get thicker and fluid thermal

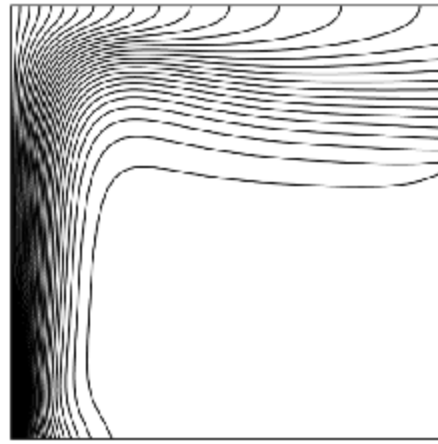
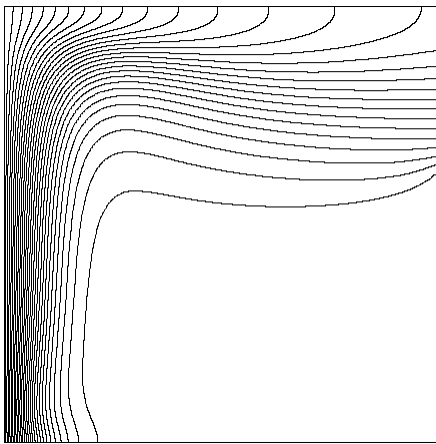
stratification in the upper region of the cavity get poorer (see isotherms in Fig. (5)), since flow of the hot fluid from the aperture is choked as the inclination is increased and that leads to slower replacement of the hot air by fresh air and that makes convection less rigorous.

4.4. Effect of Rayleigh Number

Figure (6) shows the effect of increasing Rayleigh number in the range (10^3 - 10^6) on streamlines and isotherms patterns at $H=0.8$ and $\varphi = 0^\circ$. Usually, the Rayleigh number, is defined by ($Ra = g\beta L^3 \Delta T / \nu \alpha$), and in case of using Boussinesq approximation with air as a working fluid, the ν , α and g will be constants. Thus, only β and ΔT will be the factors that govern the change in value of Rayleigh number. In case of $Ra = 10^3$, the circulation inside the cavity is so weak that the viscous forces are dominant over the buoyancy force and that leads to rather weak convection, also the effect of the open side does not seem deep in this case. Consequently, the corresponding isotherms exhibit rather slight difference as compared to those of pure heat conduction which are parallel to the surface of the thermally active part. On the other hand, when Rayleigh number increases, the buoyancy force accelerates the circulation of fluid flow and the effect of the open side penetrates further into the flow. As a result, the corresponding isotherms are greatly deformed and crowded near the active part leaving the cavity core empty. Therefore, as Rayleigh number increases, the flow becomes fully convective dominated, the fresh fluid is entrained right to the left vertical wall where high temperature gradients are created, and the discharging fluid from the upper part of the cavity occupies smaller section of the opening. It is interesting to note in case of $Ra = 10^6$, the formation of vortex in the upper portion of the cavity due to the high heat transfer rate, also the effect of the open side is quite significant in this case.



(a) $Pr = 0.71$ $Ra = 10^5$ $\phi = 0^\circ$ $H=1$



(b) $Pr = 0.71$ $Ra = 10^5$ $\phi = 10^\circ$ $H=1$

Fig. 2. Comparison of Isotherms with those of (a) Mohamad et al.[10] and (b) Nateghi and Armfield [8].

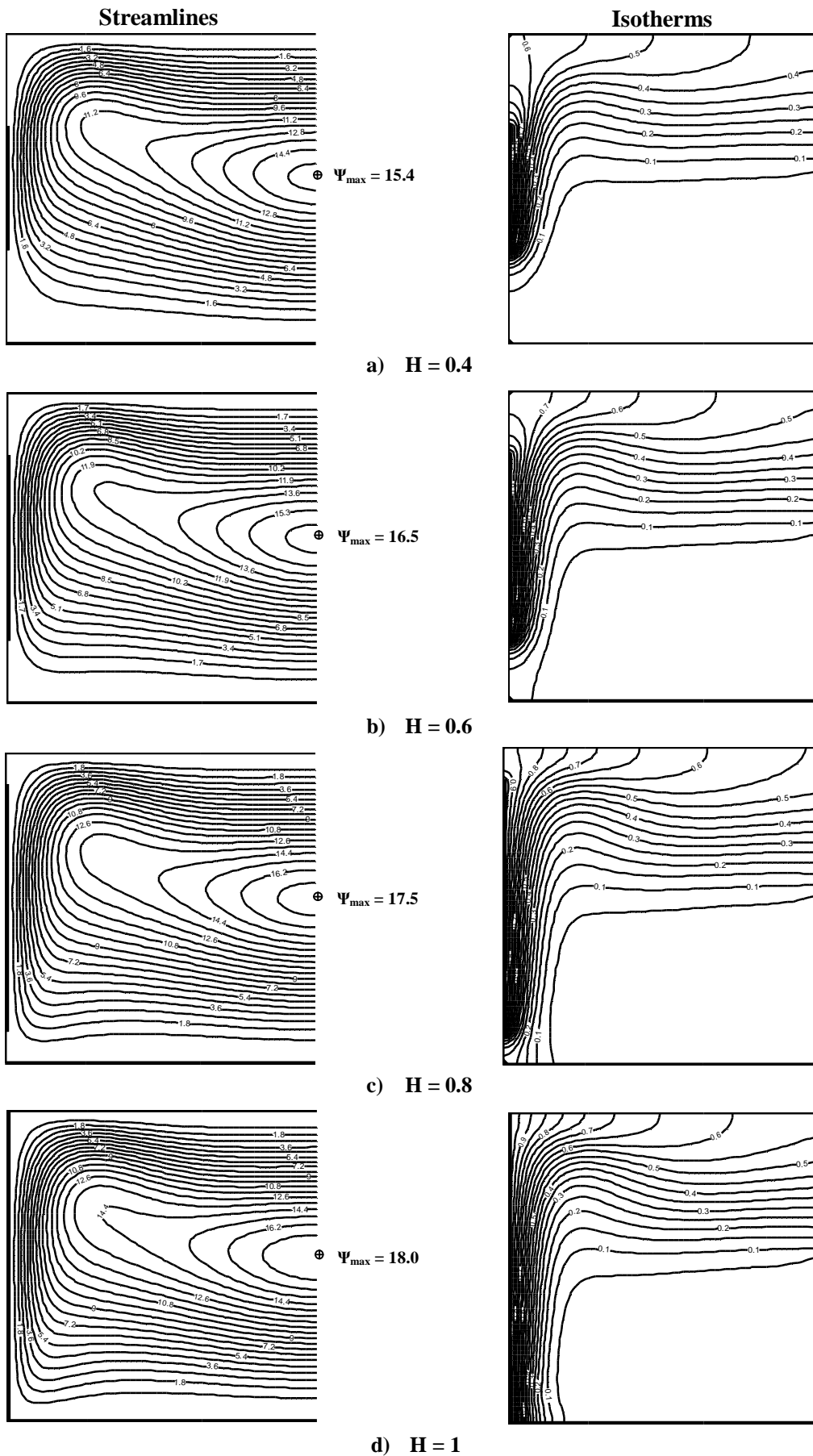


Fig. 3. Streamlines and Isothermal Contours for $\phi=0^\circ$, location of Active Part at Middle and $Ra = 10^5$, with Different Lengths of Thermally Active Part.

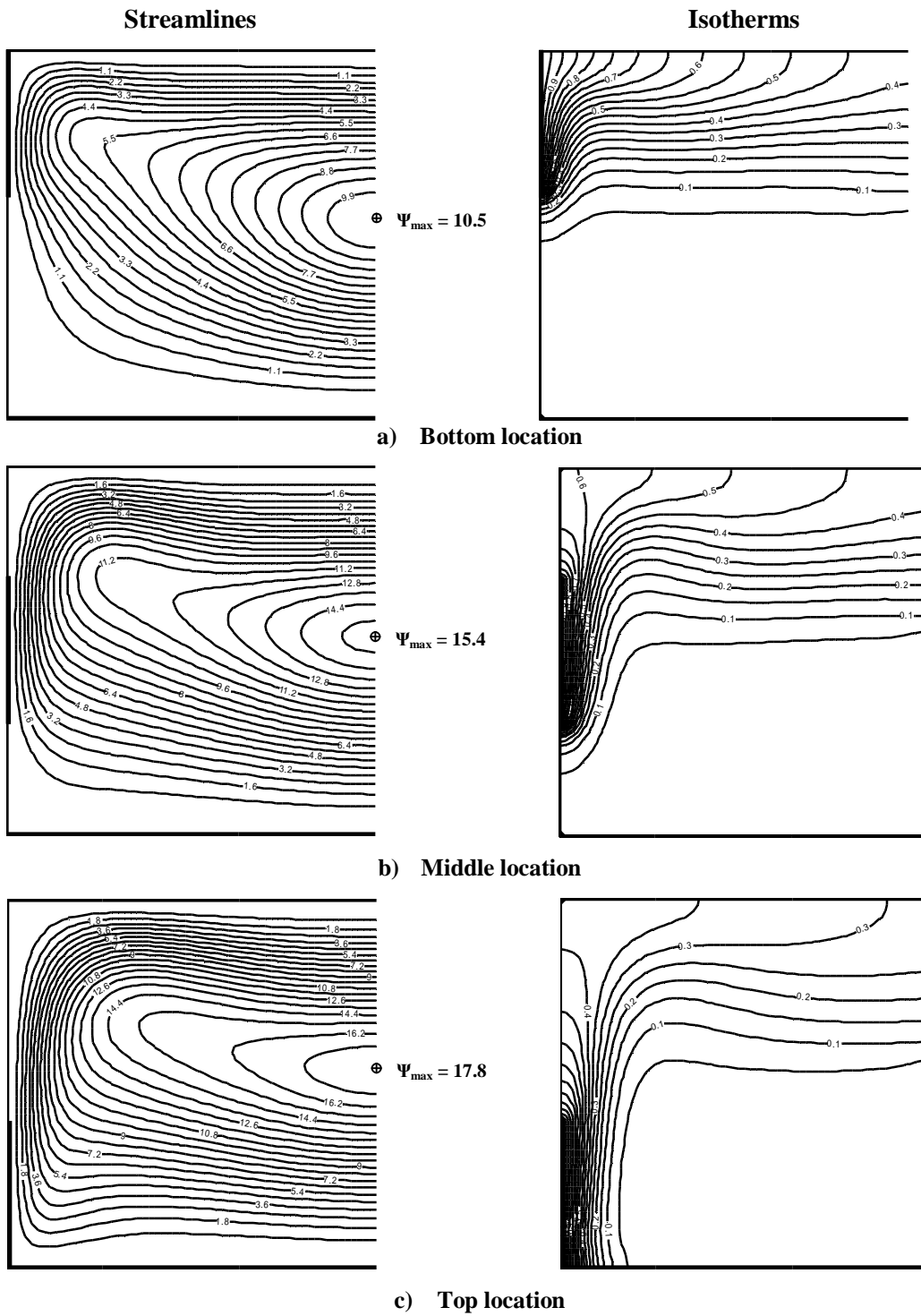


Fig. 4. Streamlines and Isothermal Contours for $\phi=0^\circ$, $H=0.4$ and $Ra = 10^5$ with Different Locations of Thermally Active Part.

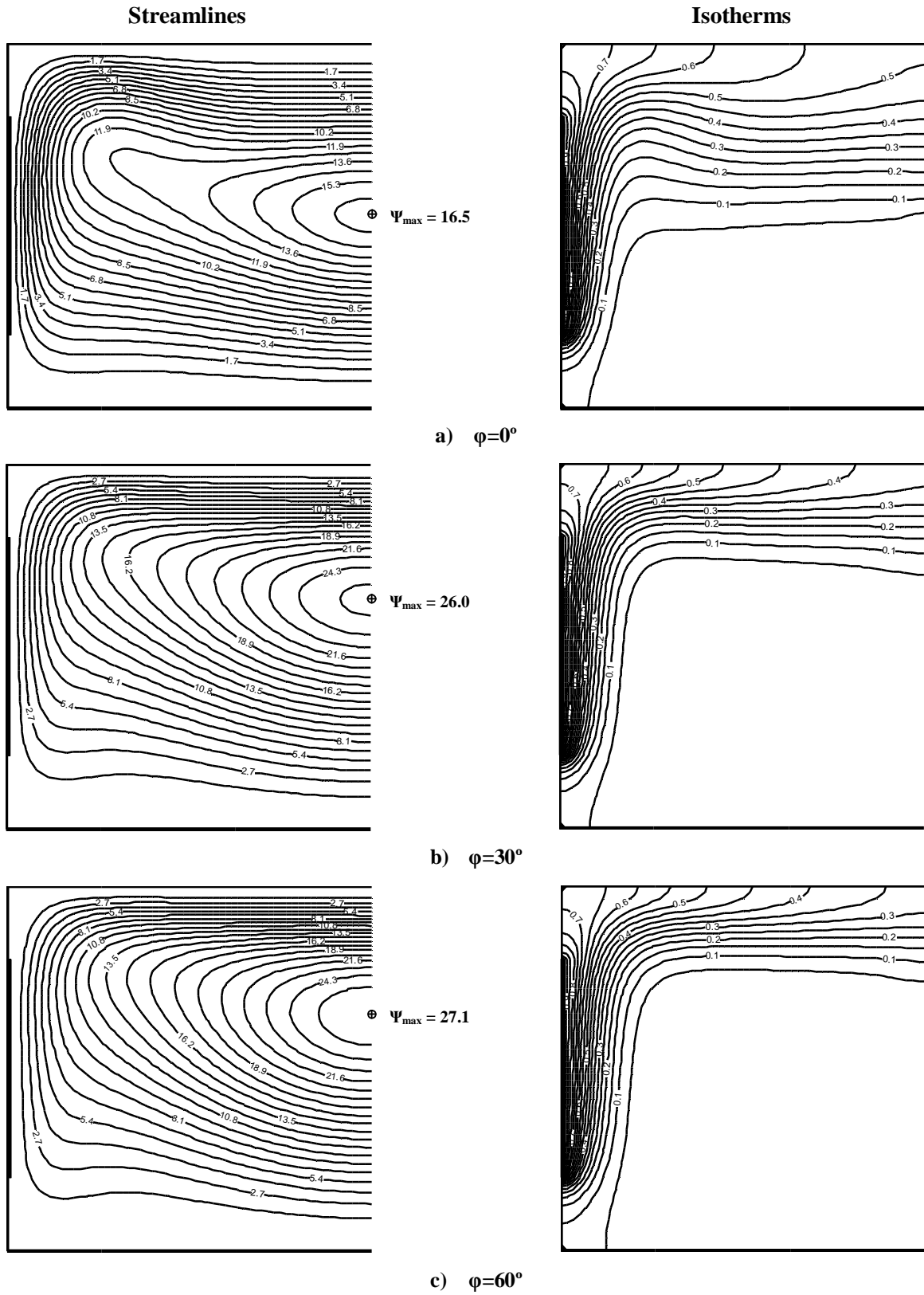


Fig. 5. Streamlines and Isotherms for H=0.6, Location of Active Part at Middle and Ra=10⁵ with Different Values of Inclination Angles.

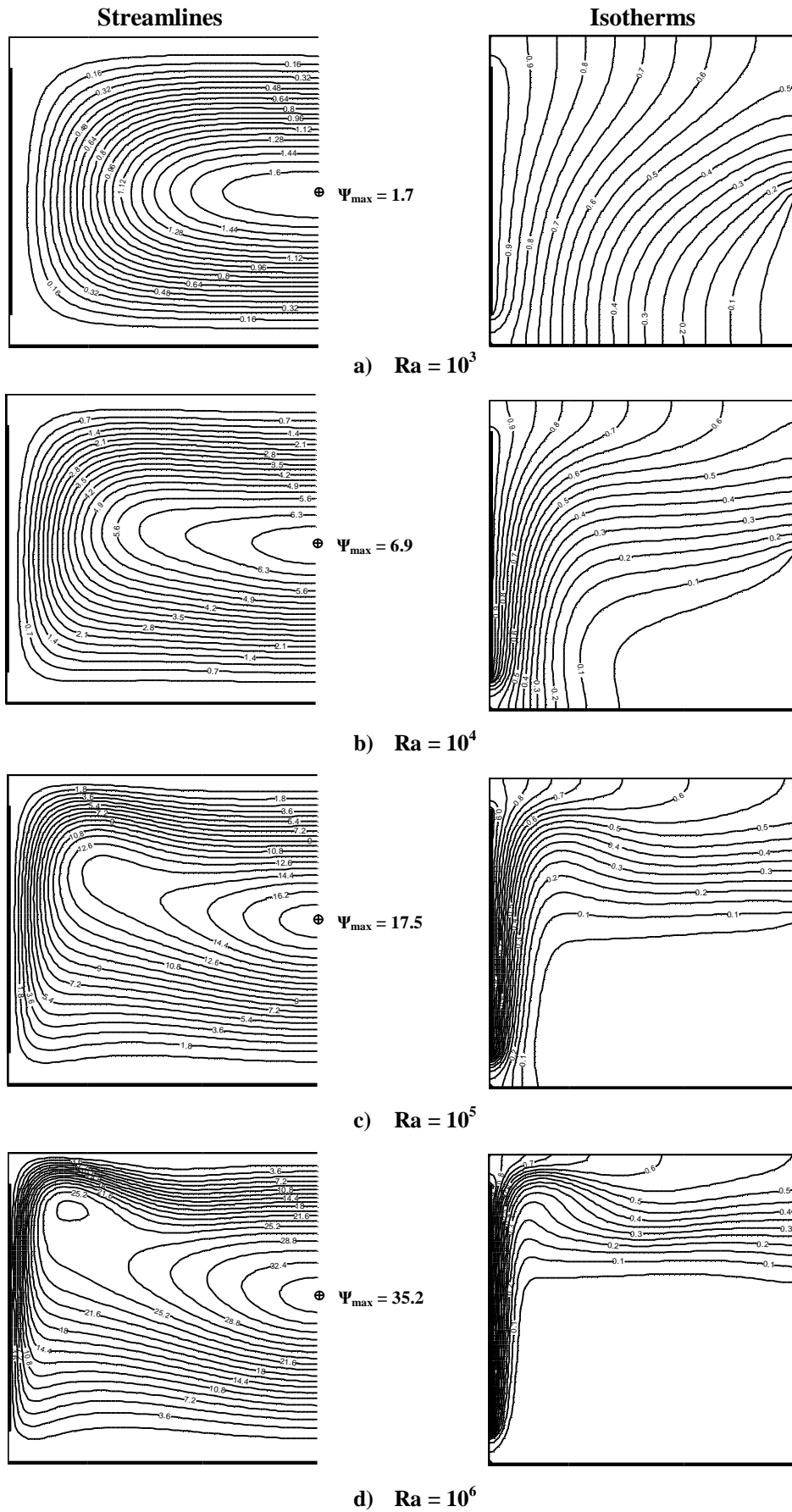


Fig. 6. Streamlines and Isotherms for $\phi=0^\circ$, Location of Active Part at Middle and $H=0.8$, with Different Values of Rayleigh Number.

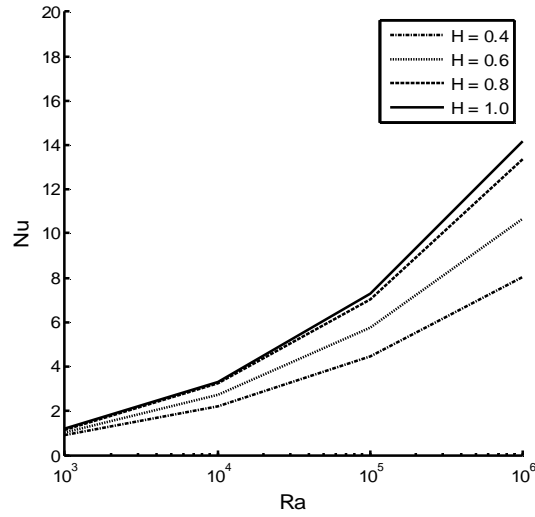


Fig. 7. Average Nusselt Number as a Function of Rayleigh Number for Different Dimensionless Lengths of Active Part at $\phi=0^\circ$ and Location of Active Part at Middle.

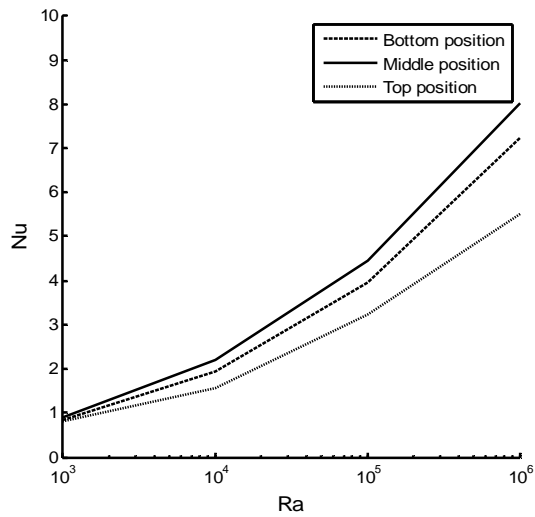


Fig. 8. Average Nusselt Number as a Function of Rayleigh Number for Different Locations of Thermally Active Part at $\phi=0^\circ$ and $H=0.4$.

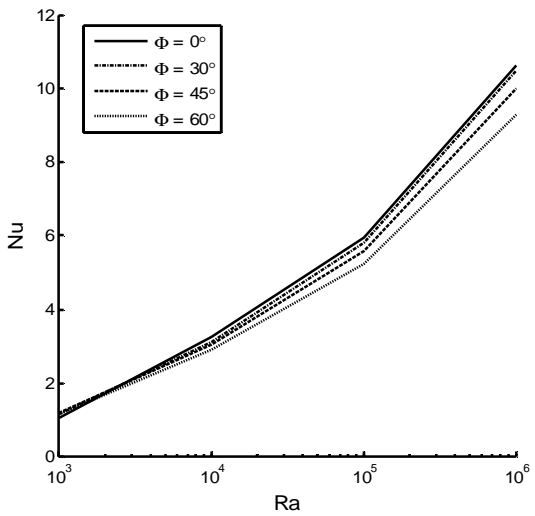


Fig. 9. Average Nusselt Number as a Function of Rayleigh Number for Different Inclination Angles at $H=0.4$ and Location of Active Part at Middle.

5. Conclusions

A steady, two-dimensional natural convection heat transfer in a square open cavity with partially active side wall has been studied numerically for different angles of inclination, different Rayleigh numbers and different lengths and locations of thermally active part. The finite-difference method was employed for the solution of the present problem. Graphical results in form of streamlines and isotherms for various parameters governing heat transfer and fluid flow were presented and discussed. The results of the present study lead to the following conclusions:

- Location and length of the active part, Rayleigh number and inclination angle are important parameters on flow and temperature fields and heat transfer in square cavity.
- Heat transfer increases with the increasing of active part length or Rayleigh number. Values of stream function (flow strength) also increase with the increasing of Rayleigh number or active part length.
- Higher heat transfer rate was obtained when the active part is at middle location in vertical wall compared to top and bottom locations.
- Increase of inclination angle increases flow strength and decreases average Nusselt number.

Nomenclature

L	length of the square cavity
g	gravitational acceleration
h	length of the active part
H	dimensionless length of the active part
s	position of the active part center
S	dimensionless position of the active part
h_y	local heat transfer coefficient
Nu	local Nusselt number
\bar{Nu}	average Nusselt number
p	pressure
T	dimensional temperature
Pr	Prandtl number (ν/α)
Ra	Rayleigh number ($g\beta L^3 \Delta T/\nu\alpha$)
x,y	dimensional Cartesian coordinates
X,Y	dimensionless coordinates
u	dimensional velocity in the x-direction
U	dimensionless velocity in the X-direction
v	dimensional velocity in the y-direction
V	dimensionless velocity in the Y-direction

Greek symbols

α	thermal diffusivity
β	thermal expansion coefficient
μ	dynamics viscosity
ν	kinematic viscosity
ω	dimensional vorticity
Ω	dimensionless vorticity
ψ	dimensional stream-function
Ψ	dimensionless stream-function
θ	dimensionless temperature
ρ	density
Δ	laplacian in Cartesian coordinates

Subscripts

∞	ambient
in	inflow
out	outflow

Superscripts

ζ	current iteration number
$\zeta-1$	previous iteration number

6. References

- [1] A. M. Clausing, Convective losses from cavity solar receivers: comparisons between analytical prediction and experimental results, *J. Solar energy* 105 (1983) 29-33.
- [2] Abdulkarim H. Abib, Yogesh Jaluria, penetrative convection in a partially open enclosure, *HTD 198 ASME* (1992) 74–83.
- [3] S. S. Cha and K. J. Choi. An interferometric investigation of open cavity natural convection heat transfer. *Exp. J. Heat transfer* 2 (1989) 27–40.
- [4] Y.L. Chan, C.L. Tien, A numerical study of two-dimensional natural convection in square open cavities, *Numer. Heat Transfer* 8 (1985) 65–80.
- [5] Y.L. Chan, C.L. Tien, A numerical study of two-dimensional laminar natural convection in shallow open cavities, *Int. J. Heat Mass Transfer* 28 (1985) 603–612.
- [6] O. Polat, E. Bilgen, Laminar natural convection in inclined open shallow cavities, *Int. J. Thermal Sciences* 41 (2002) 360–368.
- [7] Chakroun, W., Effect of Boundary Wall Conditions on Heat Transfer for Fully Opened Tilted Cavity, *ASME J. Heat Transfer*, 126 (2004) 915–923.

- [8] M. Nateghi, S. W. Armfield, Natural convection flow of air in an inclined open cavity, ANZIAM Journal 45 (2004) 870–890.
- [9] J.F. Hinojosa, R.E. Cabanillas, G. Alvarez, C.E. Estrada, Nusselt number for the natural convection and surface thermal radiation in a square tilted open cavity , Int. Communications in Heat and Mass Transfer 32 (2005) 1184–1192.
- [10] A.A. Mohamad a, M. El-Ganaoui b, R. Bennacer c, Lattice Boltzmann simulation of natural convection in an open ended cavity, Int. J. Thermal Sciences 48 (2009) 1870–1875.
- [11] N. Nithyadevi, P. Kandaswamy, J. Lee, Natural convection in a rectangular cavity with partially active side walls, Int. J. Heat Mass Transfer 50 (2007) 4688–4697.
- [12] P.J. Roach, Computational Fluid Dynamics, Hermosa, Albuquerque, New Mexico, 1985.

انتقال الحرارة بالحمل الحر في تجويف مربع مائل ذو نهاية مفتوحة و بوجود جزء نشط حرارياً

جاسم محمد مهدي

قسم هندسة الطاقة/ كلية الهندسة/ جامعة بغداد

البريد الإلكتروني: Jasim_ned@yahoo.com

الخلاصة

يصف هذا البحث دراسة نظرية لانتقال الحرارة بالحمل الطبيعي في حيز مائل مربع الشكل و مفتوح من الجانب مُحاط بجدارين علوي و سفلي معزولين حرارياً و جدار عمودي يواجه الجانب المفتوح و يحتوي الجزء النشط حرارياً الذي يكون مسخناً بدرجة حرارة أعلى من درجة حرارة المحيط. المعادلات الحاكمة لجريان المائع و انتقال الحرارة داخل الحيز مُثلت بصيغة الدوامية- دالة الجريان و تم تحويلها إلى صورة لابعدية مناسبة و من ثم فُكّت باستخدام طريقة الفروقات المحددة للوصول إلى معادلات خطية تُحل عددياً بأسلوب الإرخاء. و قد أُعدَّ برنامج حاسوبي خاص تمت صياغته ضمن برمجية الماتلاب لتنفيذ النموذج الرياضي المقترح في هذه الدراسة. وقد أمكن الحصول على التوزيع الحراري و خطوط السريان خلال الحيز و كذلك رقم نسلت المعدل و لمدى واسع من أعداد رايلي تراوحت بين ١٠-١٠٠ و زوايا ميلان تراوحت بين ٠-٦٠ درجة عن خط الأفق و لقيم مختلفة لطول و موضع الجزء النشط حرارياً. تشير النتائج التي تم الحصول عليها إلى إن معدل انتقال الحرارة يكون أعلى عند يكون الجزء النشط في منتصف الجدار العمودي مقارنة ببقية الأوضاع و يقل هذا المعدل عند زيادة زاوية ميلان الحيز. كذلك إن زيادة عدد رايلي أو زيادة طول الجزء النشط حرارياً في الجدار العمودي يؤدي إلى زيادة معدل انتقال الحرارة بالحمل الطبيعي داخل الحيز.